

DEVELOPMENT AND TESTING OF A PHYSICS-BASED MODEL
FOR THE PREDICTION OF FIRE SPREAD AND INTENSITY

W. R. Anderson, E. A. Catchpole, & B. W. Butler

FINAL REPORT OF RJVA 00-JV-11222046-501.

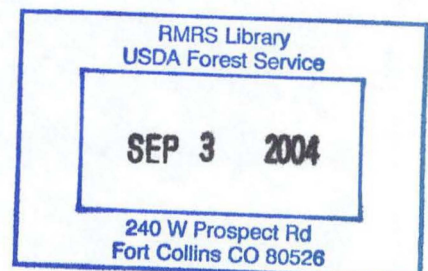
Development and Testing of a Physics-based Model for the Prediction of Fire Spread and Intensity

May, 2004

W. R. Anderson¹, E.A. Catchpole¹, and B.W. Butler²

¹Australian Defence Forces Academy,
University of New South Wales, Canberra, ACT Australia

²USDA Forest Service, Rocky Mountain Research Station,
5775 Hwy 10 W. Missoula, MT USA



FOREWORD	3
1. MODEL DEVELOPMENT	4
1.1 Ignition Temperature.....	4
1.2 Heat Transfer Mechanisms.....	6
1.2.1 Radiative Heating.....	7
1.2.2 Radiative Heat Losses	7
1.2.3 Convective heating and cooling	7
2. MODEL EQUATIONS.....	8
3. SUBMODELS.....	10
3.1 Flame Radiation Submodel	10
3.1.1 Maximum Flame Intensity	10
3.1.2 Flame Radiative Intensity — height variation.....	11
3.2 Combustion Zone Radiation Submodel	12
3.2.1 Combustion zone radiation intensity.....	12
3.2.2 Combustion zone angle	12
3.3. Flame Characteristic Models.....	13
3.3.1 Flame Angle	13
3.3.2 Flame Height	14
3.4 Convective transfer	14
3.4.1 Surface gas velocity	14
3.4.2 Gas temperature profile.....	14
3.4.2 Gas temperature characteristic distance	15
3.5 Fireline Intensity	15
4. MODEL PREDICTIONS	16
5. DISCUSSION	18
6. ACKNOWLEDGEMENTS.....	18
7. REFERENCES	19

FOREWORD

The following comprises the final report of the project organized with the objective of developing an advanced model for the prediction of fire intensity and spread. The real impetus for this effort was to develop a model that would provide increased predictive accuracy over a wider range of conditions, while including improved physics than currently available models. A second driving objective was the need to develop a model that would provide direct predictions of fire intensity in engineering variables that could serve as input for upcoming fire effects models. In other words, the fire behavior model would provide predictions of fire intensity in terms of radiant and convective energy fluxes on a spatial and temporal basis.

The effort summarized in the following pages, has consumed much of the efforts and thinking of the research team for the more than a decade. The bottom line is that wildland fire is a technically challenging problem. The combination of chemistry, radiation convection and conductive heat transfer, fluid dynamics alone comprise a difficult modelling problem. This is compounded by the spatial and temporal variation in fuel and environment through with the fire burns. Given the high level of uncertainty in our ability to define the physical conditions of the fuel and environment it is surprising that we can predict fire behaviour at all! In the end the model developed as part of this effort is not as robust as we had originally intended. The problem lies in the high dependence of many of the submodels on the fire intensity which is what we are trying to predict, so the result is that fire intensity is on both sides of the equation. The result is that the solution is at times difficult to define. However, we maintain that the experiments and subsequent analysis have resulted in significant new understanding into the physical mechanisms driving wildland fire spread and intensity. Experiments, data and techniques developed from this effort have contributed to many current research projects and will certainly affect research efforts at the Fire lab for some time into the future.

Development and Testing of a Physics-based Model for the Prediction of Fire Spread and Intensity

1. MODEL DEVELOPMENT

We develop a model for the steady spread of fire through a homogeneous fuel bed. The fuel bed is modelled as an arrangement of homogeneous particles all with the same moisture content M_f at ambient temperature. The role of the air between the fuel particles is to supply oxygen; the thermal capacity of this air is neglected.

Our model, in common with most physical and semi-physical models, concentrates on an energy balance for a small volume element containing fuel particles and air; we consider a surface volume element, as shown in Figure 1. Each element is associated with a temperature depending on its position and the time since initial ignition of the fuel bed.

The model is based on the following description of flame propagation. Combustion releases heat energy from the region of burning fuel. The unburned fuel absorbs some of this heat causing its temperature to rise. When the fuel temperature of a volume element reaches a critical value T_{ig} (the ignition temperature) the particles in the element emit ignitable gases. These are ignited by pilot ignition and the particle moves into the combustion zone, and is consumed by an exothermic combustion process. The line on the upper surface of the fuel bed separating burning fuel from unburned fuel gives the position of the fire front. This fire front propagates at a steady speed.

1.1 Ignition Temperature

During the heating process, each fuel particle is assumed to be at uniform temperature throughout its volume. For non-fine fuels this assumption is unrealistic, and modifications will be discussed later. Far away from the fire the particles are at ambient temperature but,

as the flame front approaches, the particles increase in temperature, evaporating water gradually until boiling point is reached; further heat then raises the temperature of the dry fuel element to ignition.

A crucial but frequently unstated assumption in our model, and in almost all physical models of fire spread, is that there is a well-defined ignition temperature, at which a particle bursts into flame regardless of preceding conditions. In particular, ignition takes place at this temperature regardless of how quickly or slowly the particle has been heated. Since water vapour is the first pyrolysisate, a particle heated slowly will have lost almost all moisture before ignitable gases are given off; a rapidly heated particle, or a large particle, on the other hand, will still be losing water vapour from its deeper layers while the surface is giving off ignitable gas. These gases will therefore be diluted with water vapour, and may require a higher temperature to ignite them.

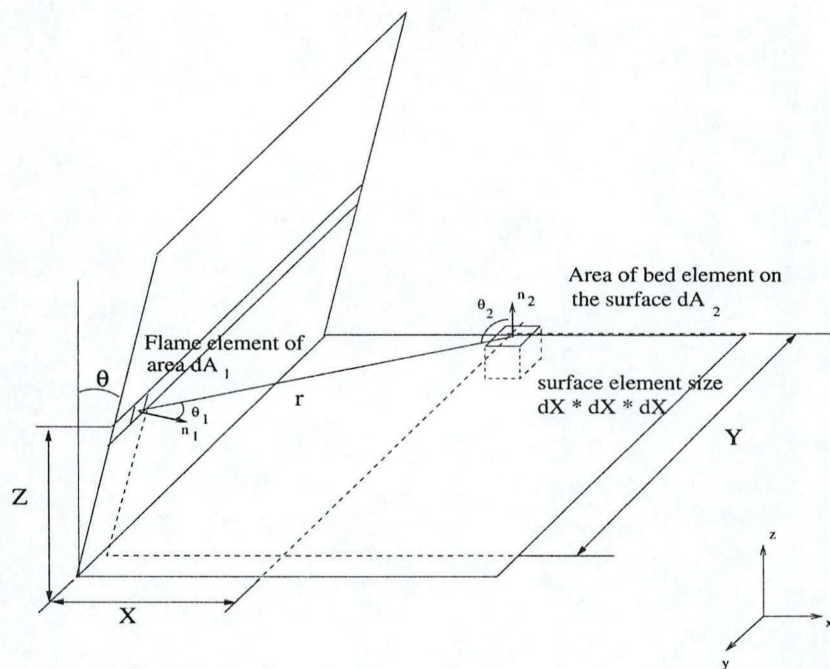


Figure 1: Schematic diagram indicating position of the fuel element on the surface of the bed.

1.2 Heat Transfer Mechanisms

Figure 2 is a schematic 2D representation of a fire moving through a fuel bed, and is used in the discussion of the fuel heating and of the submodels used to predict the various flame properties required.

The model of heat transfer from the flame to the fuel element includes radiative heating and convective heating caused by hot air from the flaming region being advected over the unburned fuel as well as radiative and convective cooling.

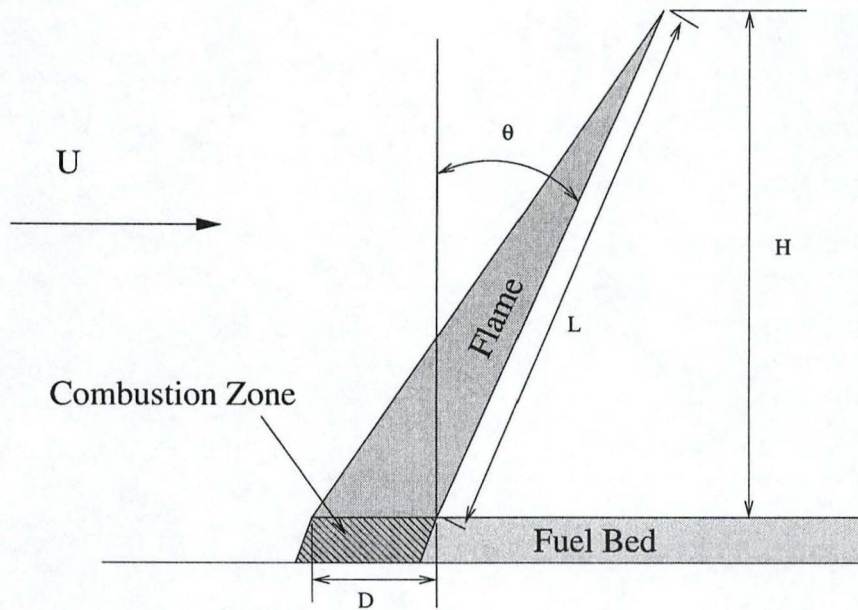


Figure 2: A two dimensional representation of a wind aided flame moving through an inclined fuel bed.

1.2.1 Radiative Heating

As with most previous models, we treat radiation from the flame as emanating from an opaque surface coincident with the average position of the front of the flame. This surface is taken to be a plane of finite length L and of finite or infinite width, inclined at an angle, θ to the vertical. The flame surface is taken to radiate as a grey body, with an emissive power varying with height above the fuel surface.

We model the radiation from the combustion zone in a similar way to that from the flame, by assuming that the combustion interface is a plane, inclined at the same angle to the vertical as the flame, but with a constant emissive power. Although combustion interfaces are known to be curved in general (Albini, 1985, 1986), the error caused by our assumption will be small in most cases, since we are considering only the heat received by a surface fuel element.

1.2.2 Radiative Heat Losses

Heat loss due to re-radiation from the element varies as $T_p^4 - T_\infty^4$, the difference between the fourth powers of the absolute temperature of the element and that of the environment.

1.2.3 Convective heating and cooling

The rate of convective heat input per unit volume of fuel bed is

$$q_c = 4\bar{h}\alpha(T_a - T_p) \quad (1)$$

where \bar{h} is the convective heat transfer coefficient, T_p is the temperature of the particles in the unit volume, and T_a is the temperature of the surrounding gas. The term $\alpha = \sigma\beta/4$ is the decay rate of radiation passing through the fuel bed (equal to the inverse of the mean free path length), σ is the particle surface area to volume ratio, and β is the fuel bed packing ratio, the fraction of the fuel bed volume that is filled with fuel. The gas may range from a mixture of air and pyrolysed gases at flame temperature, moving at fairly high

velocity and turbulent, to still air at ambient temperature (in which case q_c becomes a cooling term).

The convective heat transfer coefficient \bar{h} depends mainly on particle size and on the gas velocity. It can be calculated from empirical equations. We use a relation for forced convection (i.e. with an ambient air flow past the particle), relating the Nusselt and Reynolds numbers for a cylinder in a cross flow (Incropera and De Witt, 1985, equation 7.57).

2. MODEL EQUATIONS

Our model is based on the energy balance of a typical fuel surface volume element. The net effect of heat input and heat loss in a small interval of time is equated to the corresponding increase in internal energy of the fuel element. This energy balance leads to a differential equation for the average temperature of the volume element, which contains the rate of spread R as a parameter. We consider only the quasi-steady case where R is constant. The differential equation can be integrated as the flame front moves from the far distance (when the temperature of the volume element is ambient) towards the volume element. When the flame reaches the volume element, the temperature reaches ignition temperature and the volume element bursts into flame. This is often referred to as an integrated or global energy balance.

The differential equation for the temperature $T_p(X)$ at a distance X ahead of the combustion interface is

$$-R \rho_b c^* \frac{dT_p}{dX} = q_f(X) + q_c(X) - 4 k_r \alpha \sigma_B (T_p^4 - T_\infty^4) + 4 \alpha \bar{h}(T_a, X) (T_a - T_p) \quad (2)$$

where $T_a = T_a(X)$ is the temperature of the air or gas surrounding the particle, and $q_f(X)$ and $q_c(X)$ are the radiant heat inputs from the flame and combustion zone, respectively.

Note that q_f also depends on the bed width, flame angle and flame height, and on the emissive output of the flame, the absorptivity of the particle and α ; q_c depends on the fuel bed depth, the combustion zone interface angle, and the combustion zone emissive output, the absorptivity of the particle and α .

In (2) ρ_b is the bulk density of the fuel bed, equal to the dry mass of fuel per unit volume of fuel bed, and c^* is the average specific heat of (wet) fuel from ambient temperature to the boiling point of water, including an allowance for the latent heat of the water.

Also in (2) we have σ_B , the Stefan-Boltzmann constant, in the radiative loss term, which accounts for re-radiation from the particle. This radiative loss term is multiplied by a fraction k_r , to account for the fact that not all of the re-radiation is effectively lost by the particle. If the fuel particles below the surface were all at the same temperature as the surface element, and the fuel bed was optically thick, then there would be no net heat transfer in a downwards direction due to radiative losses, and we would have $k_r = 0.5$. If the fuel particles below the surface element were all at ambient temperature, then k_r would be 1. We assume, for the fuel beds under consideration here, that $k_r = 0.5$.

Equation 2 can be integrated directly to give

$$\begin{aligned}
 -R \rho_b Q_{ig} = & \int_0^\infty q_f(X) dX + \int_0^\infty q_c(X) dX - 4 k_r \alpha \sigma_B \int_0^\infty (T_p(X)^4 - T_\infty^4) dX \\
 & + 4 \alpha \int_0^\infty \bar{h}(T_a, X) (T_a(X) - T_p(X)) dX
 \end{aligned} \tag{3}$$

where Q_{ig} is the heat required to bring a unit mass of fuel, including its water content, from ambient to ignition temperature.

We solve equations (2) and (3) in an iterative manner. For a given value of the rate of spread R , we solve (2) to get the particle temperature field $T_p(X)$. Substituting this temperature field into (3) gives us a new value for R , and so on. However, before we can

do this, we need submodels for the air temperature field $T_a(X)$, and for the flame and combustion zone parameters (height, angle, and radiative output) that determine q_f and q_c .

3. SUBMODELS

3.1 Flame Radiation Submodel

The radiation from the flame surface to a small cubic element aligned with the top of the fuel bed surface, shown in Figure 1, is calculated as follows. The fuel bed is modelled as a collection of randomly orientated particles. Reflections from particles within the bed, which occur if the particle emissivity $\varepsilon_p < 1$, are ignored. Consider a beam of radiation from a small region dA_1 on the flame surface. Radiation enters the element through the top of the cube, the front (i.e. side closest to the flame), the back (if the fuel volume is under the flame shadow) and the two sides. Radiation passing through the element is absorbed by the fuel particles, the length of the absorbing path within the element depending on where the incident beam strikes the cube.

Calculating the energy emitted by the flame region dA_1 and absorbed by the fuel element dA_2 requires an integration over the surface of this fuel element. To calculate the total energy from the flame absorbed by the element, this must be then integrated over the whole flame surface. The second integration process requires a model for the energy flux. We assume that the flux is constant across the flame, and has a Gaussian profile in the vertical (z) direction, with a maximum value, $E_{f,0}$, at the base and a parameter, σ_G , which measures the fraction of the flame height at which radiation has decreased to 37% of the base value. Other factors having a significant influence on the flame radiation submodel are the flame angle, θ , and the flame height H ; models for these parameters are discussed in Section 3.3.

3.1.1 Maximum Flame Intensity

Laboratory flame emission flux data was measured and a Gaussian model relating emissive flux to flame height was fitted (see Butler, 1993). The maximum flame intensity, $E_{f,0}$, is best predicted by an asymptotic equation in Byram's fireline intensity, I_B , (Byram, 1959) of the form

$$E_{f,0} = a[1 - \exp(-b I_B)] \quad (4)$$

This model is approximately linear over much of the range of the data so the asymptote is not well determined. The asymptote, a , was estimated as 110 kW/sq m using data from the Canadian Crown Fire experiment that is documented in Butler *et al* (in press). The parameter b was estimated from the data as 0.00098.

The linearity causes convergence problems in the iterative process for solving equations (2) and (3). Thus, an empirical model for $E_{f,0}$ has been developed, of the form

$$E_{f,0} = p[1 - \exp(-q w_o(1 + U))] [r - \exp(-s U_2)] \exp(-t\beta) \exp(-\nu M_f) \quad (5)$$

The variables used in this empirical model are fuel loading, w_o , wind speed, U , packing ratio, β , and moisture content, M_f . The empirical constants p , q , r , s , t and ν are obtained from fitting this model to our laboratory data. The model is shown fitted to the experimental data in Figure 3. The values of the constants are $p = 63$, $q = 0.97$, $r = 1.75$, $s = 0.24$, $t = 5.4$. (Note that the asymptote is still forced to be 110 kW/sq m). The constant ν represents moisture damping which depends on the fuel type and thickness (see Catchpole *et al* 1998 for a discussion on moisture damping in the empirical model based on the laboratory data). The fitted values were $\nu = 7$ for Ponderosa pine needles, $\nu = 3.7$ for coarse excelsior, and $\nu = 0$ for fine excelsior.

3.1.2 Flame Radiative Intensity —height variation

Measuring the radiation as a function of position within the flame is extremely difficult due to the turbulent nature of the flames. We model flame radiative emissive power as

$$E_f(z) = E_{f,0} \exp \left[- \left(\frac{z/H}{\sigma_G} \right)^2 \right] \quad (6)$$

where H is the flame height and z is the height within the flame. We found no appreciable dependence of σ_G on fuel and environmental conditions, and set σ_G to be a constant equal to 0.56.

3.2 Combustion Zone Radiation Submodel

The combustion zone radiation is modelled along similar lines to the flame radiation; the major difference being that the combustion zone radiative flux, $E_{C,0}$, is considered constant over the combustion zone interface.

3.2.1 Combustion zone radiation intensity

The combustion zone emissive flux, $E_{C,0}$, can also be related to Byram's intensity, but the relationship asymptotes at a Byram's intensity (I_B) of about 500 kW/m or less. The best fit to the laboratory data is again of the form of equation (4). The model exhibits very strong linearity when I_B is less than about 300 kW/m. An alternative model, that we use, is to assume a minimum value for $E_{C,0}$, and to fit an asymptotic model. This results in the model

$$E_{C,0} = p [1 - \exp(-q I_B)] + r \quad (7)$$

where, p , q and r are empirical constants. The asymptote, r , is again chosen to be 110 kW/sq m, and from the data value of the other constants are $q = 0.00045$ and $r = 60$.

3.2.2 Combustion zone angle

Measurements of the combustion zone angle are extremely difficult to obtain and were not made for the fires in our database. Side views of the fires (using a camera close to the combustion zone) showed that, in lightly packed fuel, the combustion zone angle was close to the flame angle. Consequently our model for the combustion zone angle assumes it to be the same as the flame angle, as discussed in Section 3.3.1.

3.3. Flame Characteristic Models

3.3.1 Flame Angle

The flame angle to the vertical, θ , is assumed to depend on Byram's convection number, N_c , in the form

$$\tan \theta = a(1/N_c)^b \quad (8)$$

This dependence has been tested previously by Martin *et al* (1991) and Weise & Biging (1996). The definition of N_c is, according to Byram's original definition (Nelson 1993),

$$N_c = \frac{2gI_B}{\rho_\infty c_\infty T_\infty U^3} \quad (9)$$

where g is the gravitational constant, and ρ_∞ , c_∞ and T_∞ are the ambient air density, specific heat and temperature, respectively.

Buoyancy theory (ref) indicates that the constant, b , should be 0.5, but Nelson and Adkins (1986) found a much weaker dependence for fires in a closed wind tunnel similar to the one in which our fires were burned. The model is shown fitted to the experimental data in Figure 6. This submodel is only likely to be valid for fires in a closed wind tunnel, and should be modified for fires in the field.

3.3.2 Flame Height

The model for flame height is a modification of an approximate model given by Albini (1981) for a wind-driven fire, in terms of wind speed and Byram's intensity. The modification makes it also applicable to zero wind fires. The model is of the form

$$H = a \left[\frac{I_B}{\sqrt{U^2 + c}} \right]^d \quad (10)$$

In the case of zero-wind fires the flame height (equal to the flame length) is a function of Byram's intensity, alone. This makes it compatible with the form used for Byram's equation for flame length (Byram 1959).

3.4 Convective transfer

3.4.1 Surface gas velocity

A sensitive velocity probe measured horizontal gas velocity at the surface of the fuel bed. The measured velocities typically remained fairly constant until the probe was in the flame shadow, when they decreased (and, in the case of low wind speeds, became negative). The velocity then increased close to the flame front (either because of temperature dependence or because the probe was picking up some of the vertical buoyant velocity). Averages of the probe velocity during the approach of the fire were calculated. These averages were found to be linearly related to wind speed, and only slightly related to the fuel geometry. A simple model for surface velocity was therefore used, in which the surface velocity is a constant fraction of the ambient wind velocity.

3.4.2 Gas temperature profile

The gas temperature profile ahead of the fire is modelled as a decreasing exponential with maximum at the interface. The form of the model used is

$$T_a(X) = T_\infty + (T_{\max} - T_\infty) \exp\left(-\frac{X}{\lambda_d}\right) \quad (11)$$

Here $T_a(X)$ is the temperature of the gas at a distance X in front of the interface, T_∞ is the ambient temperature of the surroundings, T_{max} is the gas temperature at the time of ignition of the fuel particle, and λ_d is the characteristic heating distance.

3.4.2.1 Maximum gas temperature

The maximum gas temperature is modelled as a decaying exponential function of surface area to volume ratio, σ , packing ratio, β , and wind speed, U , in the form

$$T_{max} = \exp(a - b\sigma - c\beta - dU) \quad (12)$$

3.4.2 Gas temperature characteristic distance

The model for the characteristic heating distance, λ_d , is in terms of Byram's convection number, N_c , and the surface area of fuel per volume of fuel bed, $\sigma\beta$. It is of the form

$$\lambda_d = a(N_c)^b \exp(-c\sigma\beta) + d \quad (13)$$

For zero-wind fires this reduces to a constant characteristic heating distance d .

3.5 Fireline Intensity

Many of the submodels require Byram's intensity, defined as $H_c w_a R$, where H_c is the fuel heat content, w_a is the mass of fuel consumed per unit area of fuel bed, and R is the spread rate. As flaming combustion is of primary interest, the heat content of the volatiles, H_v , is used as the heat content, and the fuel consumed is that consumed in flaming combustion. The heat content of the volatiles for the fuels used was determined from Susott (1982). It varied only slightly between fuels, and an average value of 14600 kJ kg^{-1} was used.

For the laboratory data, efficiency (fraction of fuel consumed in flaming combustion) was reasonably constant at 0.93 for the milled wood. For the pine needles, efficiency, η , was governed by moisture content, M_f . The fitted equation was of the form

$$\eta = a \exp(-bM_f) \quad (14)$$

4. MODEL PREDICTIONS

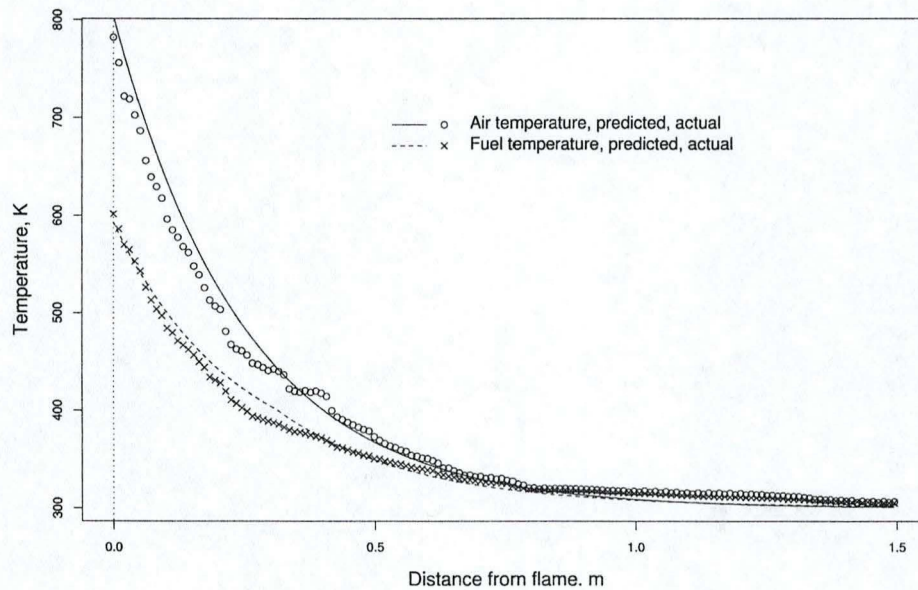


Figure 3: Comparison of the predicted and measured air and fuel temperature profiles for a typical fire experiment.

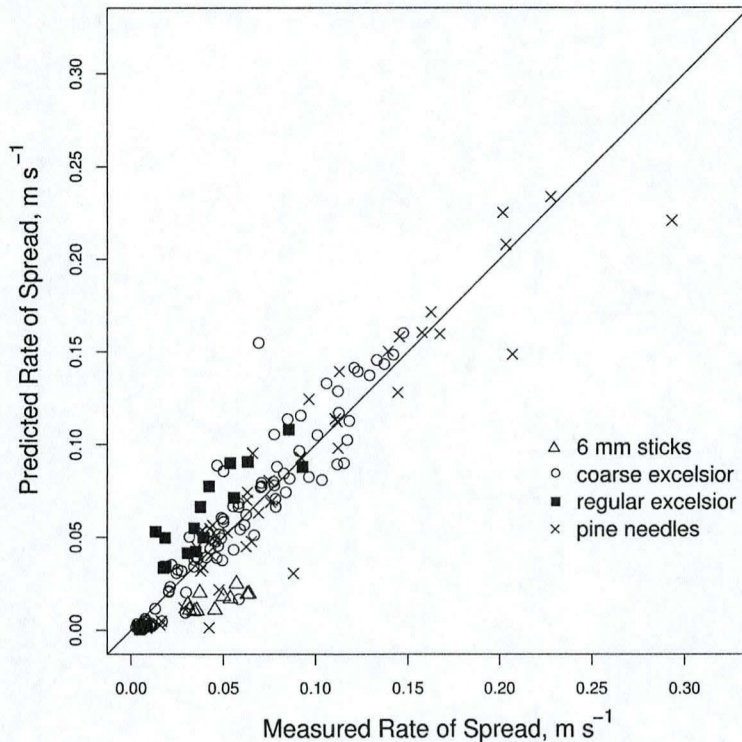


Figure 4: Comparison of the predicted and measured rate of spread.

Figure 3 shows the measured and predicted air and fuel temperature profiles for a typical fire experiment. Both the air and fuel temperature profiles show good agreement with the data. Figure 4 shows a comparison of the measured rates of spread with those predicted using the model developed in this paper. The agreement between the measured and predicted rates of spread is generally quite good, although there are a number of fires for which the agreement is poor. The fires, for which we have poor predictions, fall into two broad categories, those with both low load and low packing ratio, and those with zero wind. We acknowledge that problems exist with the model at zero wind and we are currently working to eliminate this. The poor low load/packing ratio fires are probably due

to nature of the fire itself. Under these conditions it is difficult to describe a fire front as the combustion appears discontinuous and moves from individual fuel element to fuel element.

5. DISCUSSION

As shown in Figure 4 the model works well on laboratory data for wind aided fires on flat beds. The submodels are currently being modified to predict spread rate for the laboratory fires in zero wind and on slopes. To predict spread rate in the field we may need to modify the flame characteristic submodels, as the parameters of the relationships may be different when buoyancy is not limited by the wind tunnel roof. We also need the submodels to incorporate the effect of fireline width, mixed size classes, live fuel, and the combined effects of wind speed and slope. These models are currently being developed.

6. ACKNOWLEDGEMENTS

Funding for this effort was provided by the Joint Science Fire Program, the USDA Forest Service and the University of New South Wales. Patricia Andrews deserves the sincere appreciation of the research team for her support and efforts to find funding for the project and to provide technical advice and insight whenever needed. The project would never have occurred without the early efforts and support of Richard Rothermel. Dick was the driving influence for the initiation of this work. His work and efforts to develop methods and models for predicting fire spread and intensity formed the foundation from which this work was developed. He has since retired and moved on to other projects, but his influence is evident everywhere within this work. A large part of this effort consisted of hundreds of experiments conducted in the Missoula Fire Sciences Laboratory Combustion Chamber and Wind tunnel. These experiments benefited from the dedication and expertise of the numerous personnel working at the Lab. They include Bob Schuette, Paul Sopko, Merlin Brown, Glen Morris, and Kyle Shannon.

7. REFERENCES

- Albini, F. A. 1981. A model for the wind-blown flame from a line fire. *Combustion and Flame* 43: 155-174.
- Albini, F.A. 1985. A model for fire spread in wildland fuels by radiation. *Combustion Science and Technology* 42: 229-258.
- Albini, F.A. 1986. Wildland spread by radiation – a model including fuel cooling by convection. *Combustion Science and Technology* 45: 101-113.
- Butler, B.W. 1993. Experimental measurements of radiant fluxes from simulated wildfire flames. In *Proceedings of the 12th Conference of Fire and Forest meteorology*. Jeckyll Island, GA. Bethesda:SAF publications.
- Butler, B.W., Cohen, J., Latham, D.J., Schuette, R.D., Sopko, P., Shannon, K.S., & Jimenez, D. (in press) Measurements of emissive power and temperature in crown fires.
- Byram, G.M. 1959. Forest fire behaviour. In Brown, A.A. & Davis, K.P. *Forest fire: control and use*. New York: McGraw Hill.
- Catchpole, W.R., Catchpole, E.A., Butler, B.W., Rothermel, R.C., Morris, G.A. & Latham, D.J. 1998 Rate of spread of free-burning fires in woody fuels in a wind tunnel. *Combustion Science and Technology* 131: 1-37.
- Incropera, F.P & DeWitt, D.P. 1990. *Fundamentals of heat and mass transfer*. 3rd Edition. New York: Wiley.
- Martin, R.E., Finney, M.A., Molina, D.M., Sapsis, D.B., Stephens, S.L., Scott, J.H., & Weise, D.R. 1991. Dimensional analysis of flame angles versus wind speed. In Andrews, P.L. & Potts, D.F. (eds.) *Proceedings of the 12th Conference of Fire and Forest meteorology*. Missoula, MT. Bethesda; SAF publications.
- Nelson, R. M. and Adkins, C. W. (1986). Flame characteristics of wind-driven surface fires. *Canadian Journal of Forest Research* 16, 1293-1300.
- Nelson, R.M. 1993. Byram's derivation of the energy criterion for forest and wildland fires. *International Journal of Wildland Fire* 3: 131-138.
- Rothermel, R.C. 1992. A mathematical model for predicting fire spread in wildland fuels. USDA Forest Service, Intermountain Forest and Range Experimental Station, Ogden, UT, Research Paper INT-115.
- Sussot, R. 1982. Characterisation of the thermal properties of forest fuels by combustible gas analysis. *Forest Science* 28: 404-420.
- Weise, D.R. & Biging, G.S. 1996. Effects of wind velocity and slope on flame properties. *Canadian Journal of Forest Research* 26: 1849-1858.